Microalgal food sources greatly improve macroinvertebrate growth in detritus-based headwater streams: Evidence from an instream experiment

Tiphaine Labed-Veydert, Michael Danger, Vincent Felten, Alexandre Bec, Martin Laviale, Maria Cellamare, Christian Desvilettes

Title: Microalgal food sources greatly improve macroinvertebrate growth in detritus-based headwater streams: Evidence from an instream experiment

Running head: *Microalgae boost invertebrate growth in streams*

Authors: Tiphaine Labed-Veydert[1], Michael Danger[2,3,], Vincent Felten[2], Alexandre Bec[1], Martin Laviale[2], Maria Cellamare[4], Christian Desvilettes[1]

[1] Université Clermont Auvergne, UMR CNRS 6023, Laboratoire Microorganisme, Génome, Environnement, Impasse Amélie Murat, 63170 Aubière

[2] Université de Lorraine, CNRS, LIEC, F-57000 Metz, France

[3] Institut Universitaire de France (IUF), Paris, France

[4] Phyto-Quality, Paris, France

Correspondance to: C. Desvilettes, christian.desvilettes@uca.fr

Key words:

Nutritional quality, Compound-Specific Stable Isotopes, epilithic biofilms, *Gammarus pulex*, *Rhithrogena semicolorata*

Abstract:

1. In forested headwater streams, inconspicuous food resources such as epilithic microalgae can play a major role due to their content of long chain polyunsaturated fatty acids (FAs) that are essential for macroinvertebrate development. Yet, the use of these resources and their consequences for consumers and life history traits remain scarcely studied, especially for non-herbivorous taxa.

2. Using in instream mesocosms, we aimed to understand how two macroinvertebrate species, a shredder detritivore (*Gammarus pulex*) and a scraper (*Rhithrogena semicolorata*), use available organic resources under light versus shaded conditions (high and low amounts of phototrophic biofilm, respectively). We specifically focused on the origin of carbon and essential lipids (polyunsaturated FAs, sterols) assimilated by the two species and the effects of these compounds on their survival and growth.

3. When autotrophic biofilms were available (mesocosms exposed to light), both species experienced significantly higher growth than in mesocosms placed in the dark. In *Rhithrogena* nymphs, the survival and imago emergence rates were positively affected by access to autotrophic biofilms.

4. Using stable isotope analysis ($\delta^{13}C$ & $\delta^{15}N$), we demonstrated that under dark conditions both macroinvertebrates assimilated carbon of detrital origin. Under light conditions, most of the carbon assimilated by *R. semicolorata* was derived from autotrophic biofilms and around 11% from fine detrital particles (FPOM). *G. pulex* derived part of its carbon from detrital sources (mainly FPOM) and from autotrophic biofilms.

5. The results of isotopic analyses ($\delta^{13}C$) on fatty acids and sterols showed that the scraper *Rhithrogena* was entirely dependent on autotrophic biofilms to meet its dietary FAs and sterol requirements. In contrast, detrital sources were quantitatively important for *G. pulex* both in terms of carbon and sterol supply, irrespective of the conditions tested. For these consumers, microalgae seemed to be a complementary food source, but yet essential to cover a large part of their requirements in long chain polyunsaturated FAs.

6. This study clearly confirmed the ecological importance of autotrophic biofilms for two representative functional feeding groups of macroinvertebrates in headwater streams providing new insights on the trophic origin of sterols and long chain polyunsaturated FAs in their diet.

Introduction

In temperate regions, headwater stream invertebrates obtain energy from a limited number of organic sources defined either as allochthonous (e.g., leaf litter from riparian vegetation) or autochthonous (epilithic and periphytic biofilms) (Allan & Castillo, 2007). While leaf litter can be quantitatively dominant in the diet, (Collins et al., 2016), it is typically considered to be of poor nutritional quality (Tank et al., 2010). One of the main limitations of the nutritional value of leaf litter is the lack of long-chain polyunsaturated fatty acids (LC-PUFAs) 20:5ω3, 20:4ω6 (Torres-Ruiz et al., 2007; Brett et al., 2017), regardless of the leaf palatability, which is a function of the tree species considered. Undoubtedly, microorganisms and hyphomycetes colonizing submerged leaves increase nutritional quality by reducing stoichiometric imbalances (Danger et al., 2013), but they do not increase LC-PUFA contents, which remain limited to the presence of 18:2ω6 and 18:3ω3 compounds (Torrez-Ruiz et al., 2007). In contrast, the nutritional importance of autotrophic biofilms for stream invertebrates has only recently been highlighted (Guo et al., 2016a) and this is in part due to the higher polyunsaturated fatty acid (PUFA) content of microalgae found in biofilms. LC-PUFAs are particularly abundant in epilithic diatoms in headwater streams (Cashman et al., 2013; Honeyfield & Maloney, 2015; Guo et al., 2016a). Diatoms can also contain sterols in sufficient nutritional quantity for a number of aquatic invertebrates (Gergs et al., 2015), making microalgae a high quality nutritional resource. Over the past decade, studies of numerous aquatic invertebrate species have highlighted the importance of dietary LC-PUFAs (20:5ω3, 20:4ω6) for their survival, somatic growth and reproduction (Ahlgren et al., 2009; Aguilar et al., 2012; Guo et al., 2016a; Crenier et al., 2017). The LC-PUFAs 20:4ω6 and 20:5ω3 are considered "essential nutrients" in the sense that their bioactive nature has a positive effect on invertebrate growth or other biological responses (Tocher et al., 2019). Macroinvertebrates are therefore expected to recover most of their essential lipid compounds, or even most of their carbon, from microalgae (Brett et al., 2017). Consumption of microalgae rich in 20:5ω3 and sterols that are precursors of cholesterol synthesis can improve somatic growth in both invertebrate shredders and grazers (Guo et al., 2016a; Martin-Creuzburg & Merkel, 2016; Crenier et al., 2017), provided there is sufficient algal biomass (Kühmayer et al., 2020). This last

condition is important because shading in headwater streams can severely limit biofilm growth, in turn limiting invertebrate access to sufficient levels of LC-PUFAs (Hill et al., 2001; Honeyfield & Maloney 2015). It is therefore necessary to determine of resource use when primary production is temporally limited or markedly reduced in forested streams (Alberts et al., 2018; Torrez-Ruiz et al., 2019). Most of the carbon and fatty acids (FA) and even sterols, in invertebrate diets, are derived from microalgae when epilithic biofilms and/or litter biofilms are well developed (Kühmayer et al., 2020). If biofilm development is limited, allochthonous sources will be more important for carbon supply, with microalgae being a secondary food source. Limited access to LC-PUFAs could then become a trophic constraint for macroinvertebrates, the importance of which probably depends on their functional feeding group (FFG) and stage of development.

In this context, the aim of our study was to evaluate the use of allochthonous and autochthonous organic sources by two macroinvertebrates species commonly found in temperate headwater streams in Europe, and belonging to contrasting FFGs: the amphipod shredder *Gammarus pulex* and the grazer-scraper *Rhithrogena* (*semicolorata*-group; Heptageniidae). An experiment was carried-out in early summer under semi-natural conditions, using instream mesocosms placed under either naturally light or dark conditions thereby enabling the development of predominantly autotrophic or heterotrophic biofilms, respectively. Our main objectives were: 1) to understand the origin of carbon and essential lipids (LC-PUFAs, sterols) assimilated by the two species according to their level of access to autotrophic biofilms, and then 2) to assess the impact of essential lipids on their growth and development. We used stable-isotope ratios (δ13C and δ15N) to estimate the relative contributions of organic sources to the bulk carbon assimilated by both species. Assuming that δ^{13}C values differed sufficiently between organic sources then it should be possible to reveal the relative influence of different sources on the diet assimilated by consumers (Caroll et al., 2016). To trace the origin of PUFAs and sterols, we used stable compound-specific isotope analysis (CSIA).

Materials and methods

Experimental devices and procedures

The experiment was performed from 20 June to 11 July 2018 on a controlled-flow reach of the Desges River, a fourth-order stream located in the French Massif Central (Alt: 511m; 45°4'43.84"N - 3°31'55.57"E). Six mesocosms were arranged in two blocks of three: one block was exposed to natural light whereas the other block was placed 30 m upstream and kept in the dark using an opaque tarpaulin stretched across the reach. The reach presented an homogeneous morphology (depth: 0.5 m; width: 1.40 m) with sandy substrate and the two blocks of mesocosms were separated by a short distance (30 m) minimising any differences between blocks/treatments associated with stream slope, altitude or similar variables. So, although the light treatment was confounded with the spatial location of blocks in this design, differences in other conditions between the two blocks are likely to be small compared to the treatment effect.

Water quality was monitored during the survey using AFNOR guidelines (AFNOR, 1990). Its physico-chemical characteristics were as follows: pH = 7.2, Silicate = 11.4 ± 0.4 $mg.L^{-1}$, P_{total} = 28 ± 1$\mu g.L^{-1}$ and N_{total} = 725 ± 25 $\mu g.L^{-1}$. Data loggers (HOBO™, PCE Inst., Soultz, France) were used to record the level of light and the temperature inside the flumes and in the reach every hour throughout the experiment. The mesocosms, manufactured by AOT-Plastics® (Thiers, France), comprise a plexiglass flume (L x W x H: 1 x 0.25 x 0.25m) fitted with two movable grids (mesh sizes: 250 µm) for water inlet and outlet and a dorsal hatch that can be fitted with an emergence trap. For our experiment, the bottom of the flume was covered with quartz gravel for invertebrate shelter and ceramic tiles (10 ×10 cm) were placed on the gravel to allow autotrophic (light conditions, LC) or heterotrophic (dark conditions, DC) biofilm to develop over a period of three weeks. Four coarse-meshed litter bags (mesh size 10 mm), each containing 6 grams of dry Alder leaves (*Alnus glutinosa;* harvested the previous fall) were also implanted in each flume to be microbially-conditioned over the three-week period.

On the day before the start of the experiment, *Gammarus pulex* were collected from a small tributary of the Desges river and *Rhithrogena semicolorata* nymphs were collected from the upstream part of the Desges river. The macroinvertebrates were separated into six groups

containing 100 *G. pulex* of homogeneous size (4.94 ± 0,99 mm) and 43 *R. semicolorata* nymphs (6.33 ± 1.41 mm) in similar stages with developing wing pads. At T0, a batch of 100 *G. pulex* and 43 *R. semicolorata* was introduced into each mesocosm. Maintenance of the flumes was carried out every two days and *R. semicolorata* emerged imagos were counted every three days.

Sampling

Sampling of basal sources was carried out at the beginning (T0: June 20) and at the end (T20: July 9) of the experiment. For each replicate, leaf material in the flume was removed from two litter bags and rinsed to remove fine debris and potential micro-invertebrates. Sub-samples of leaf material were used for lipid and stable isotope analysis and stored at – 80°C. The fine shredded leaf debris were sieved through a stack of filters with different mesh sizes, yielding the fine particulate organic matter FPOM (fraction 0.10 to 2 mm). FPOM was concentrated on a GF/A filter and frozen at -80°C prior to further analysis. In each replicate flume, ceramic tiles were taken at random and scraped with a toothbrush in order to recover the biofilm microorganisms. During the experiment, a biofilm gradually developed on the plexiglass walls in LC only and was collected from a 169 cm^2 wall surface on each LC flume. The biofilms were divided into sub-samples, half of which was filtered on GF/F filters and frozen at -80°C prior to further analyses, and the other half fixed with a lugol solution for microalgae identification and enumeration.

At T0, an initial batch of macroinvertebrates, similar to those introduced into the plexiglass flumes, was kept for analysis. One subsample of 30 *G. pulex* or *R. semicolorata* was fixed in 70% ethanol to determine initial size measurements. Three triplicates of 10 *G. pulex* and 5 *R. semicolorata* were frozen at -80°C prior for lipid and stable isotope analysis (SIA). At the end of the experiment (T20), all the invertebrates were collected from each flume, counted and separated into sub-samples. Depending on the number of survivals, *G. pulex* (DC: 3 x 8; LC: 3 x 10) and *R. semicolorata* (DC: 3 x 4; LC: 3 x 4) were fixed in 70% ethanol to determine their respective final sizes and gut contents. In both tested conditions the remaining macroinvertebrates were kept for 24 hours in filtered reach water to empty their digestive tracts, divided into triplicates of 3 to 5 individuals each, and frozen at -80°C prior to SIA and lipid analysis.

188

189

190 *Survival and macroinvertebrate growth analysis*

191 Survival was calculated from living invertebrates collected at the end of the experiment minus
192 sampled individuals or emerged subimagos (in the case of *R. semicolorata*). *G. pulex* were
193 photographed under a stereomicroscope (×6 to ×40 magnification) in their curved state. Length
194 was recorded from the base of the first antenna to the base of the telson using SigmaScan Image
195 Analysis Version 5.000 (SPSS Inc, Chicago, IL, USA; linear state = 0.88 × curved state [mm]; r^2 =
196 0.98). Total body length of *R. semicolorata* (not including cerci) was measured under a
197 stereomicroscope.

198

199 *Basal sources*

200 Leaf mass remaining in each bag (n=4) was weighed and compared to the initial mass. Leaf
201 litter decomposition rates (*k*) in both treatments were estimated using an exponential model (m_r =
202 $m_0 \times e^{-kt}$), where m_r is the leaf mass remaining at t (T20) and m_0 is the initial leaf mass. The
203 counting of biofilm microalgae and taxonomic identification were undertaken using an inverted
204 microscope following the Utermöhl method. Cell measurements were carried out using a digital
205 camera and an image analyser software (Zen 2, C. Zeiss GmbH, Göttingen, Germany) and the
206 results were expressed in terms of biovolume ($\mu m^3.cm^{-2}$).

207

208 *Macroinvertebrate diet analysis*

209 The diet composition of both species at the end of the experiment was determined by gut
210 content analyses using the method of Felten et al. (2008). Briefly, foregut contents were placed
211 into a drop of water on microscope slides, homogenized, then examined at different
212 magnifications from 100x to 400x to assess the approximate percentage by area of the six items
213 recorded: (i) animal matter, (ii) FPOM (fine amorphous detritus lacking well-defined cellular
214 structure), (iii) diatoms, (iv) filamentous algae, (v) CPOM (coarse particulate organic matter:
215 mainly leaf detritus with brownish palisade cell layers), and (vi) small mineral particles.

216

Bulk stable isotope analysis

All samples for bulk stable carbon and nitrogen isotope analysis were oven-dried at 60°C for 24h-48h, then ground, homogenized, and weighed in a tin capsule. Samples were prepared in triplicate for each condition and injected into a Carlo Erba NC2500 Elemental Analyzer (Milan, Italy) linked to a Thermo Finnigan Delta Plus Mass spectrometer (Les Ullis, France). Isotopic ratios were presented as δ values (‰) expressed relative to the atmospheric N_2 and Vienna Pee-Dee Belemnite for nitrogen and carbon, respectively. Analytical precision (based on the standard deviation of replicates of internal standards) was never > 0.4‰ and 0.23‰ for nitrogen and carbon respectively.

Lipid analysis: FA and sterols

All samples were freeze-dried before lipid analysis. The FA composition was determined from total lipids (TL) for basal organic sources and from neutral lipids (NLFA) and polar lipids (PLFA) for *G. pulex* and *R. semicolorata* nymphs. Lipids were extracted and when necessary fractionated using pre-packed silica columns (SPE Strata NH2 Phenomenex®, Le Pecq, France) following the methods described by Koussoroplis et al. (2010). FAs from lipid extracts were converted into FA methyl-esters (FAME) by acid-catalyzed transfersterification (Koussoroplis et al., 2010). FAME were separated and analyzed using an Agilent 6850 gas chromatograph (Les Ullis, France) equipped with a J&W DB-WAX capillary column (Agilent, 30 m × 0.25 mm). Individual FAME were identified by comparing retention times with certified commercial standard mixtures and quantified using 13:0 and 23:0 as internal standards. The identification of all peaks was confirmed or refined using an Agilent 6850 GC coupled to a 5975B Agilent Mass Spectrometer (Les Ullis, France). FAME Spectra separated with a DB wax column were identified using the reference libraries and databases available (NIST/NBS; lipidhome). Analysis of the sterols was undertaken using total lipid extracts obtained from the macroinvertebrate samples and from basal sources. Lipids were saponified with 0.2 $mol.L^{-1}$ methanolic KOH. Then, the unsaponifiable material was extracted with hexane - diethyl ether, following the detailed procedure of Gergs et al. (2015). After

derivatization by silylation, sterol TMS ethers were analyzed by GC-MS using an Agilent 6850 GC coupled to a 5975B Agilent mass spectrometer and equipped with a J&W HP-5MS (Agilent, 30 m × 0.25 mm) capillary column. Each sterol was identified by its mass spectrum and quantitation was carried out using 5α-cholestane as an internal standard and calibration curves generated with our different laboratory standard sterols.

Compound-Specific Isotope Analysis (CSIA)

The stable carbon isotope signatures (δ^{13}C values) of FAME and sterol TMS ethers were determined using a Thermo Trace 1310 GC interfaced with a Thermo Finnigan MAT 253 IRMS (Les Ullis, France) via a GC IsoLink II combustion interface. FAME were separated using an Agilent DB-FATWAX capillary column (30m x 0.25mm ID x 0.25 mm film) while sterol TMS ethers were separated in a nonpolar DB-5ms capillary column (60m x 0.25mm ID x 1 mm film). All the isotope values were reported using the δ notation relative to the Vienna Pee-Dee Belemnite reference standard. The measured δ^{13}C values were corrected by isotopic mass balance for contributions of carbon incorporated during derivatization of FA and sterols. FAME δ^{13}C values were corrected using the formula:

$$\delta^{13}C_{FA} = \frac{[(n+1) \times \delta^{13}C_{FAME} - \delta^{13}C_{MeOH}] - 1}{n}$$

where $\delta^{13}C_{FAME}$ and $\delta^{13}C_{MeOH}$ are the δ^{13}C values of the measured fatty acid methyl ester and methanol used during methylation, respectively. $\delta^{13}C_{FA}$ represents the FA δ^{13}C before its methylation, and n is the number of carbon atoms in the non-methylated FA.

Sterol δ^{13}C values were corrected using the formula:

$$\delta^{13}C_{sterol} = \frac{[(nCsterolTMS \times \delta^{13}C_{sterolTMS}) - (3 \times \delta^{13}C_{TMS})]}{nCsterol}$$

where $\delta^{13}C_{sterolTMS}$ and $\delta^{13}C_{TMS}$ are the δ^{13}C values of the measured sterol TMS ether ester and BSTFA used during silylation, respectively. $\delta^{13}C_{sterol}$ represents the sterol δ^{13}C before its silylation, and n is the number of carbon atoms in the sterol and its sterol TMS counterpart.

Data analysis

All statistical analyses were carried out using Rstudio and open source R packages (Version 1.1.456 – © 2009-2018 RStudio, Inc.). The normality and homoscedasticity of the data were tested with the Shapiro-Wilk and Levene tests, respectively. Diets and performance parameters of both macroinvertebrate species were compared between treatments using a proportion test (prop.test Z) while growth parameters were compared with a Mann-Whitney *U*-Test. Biochemical compound data (FA, sterols, δ^{13}C values) were analyzed between and within treatments. Depending on the data distribution, a Mann-Whitney U-Test or a Student t-test was applied to compare paired samples. A one way- ANOVA followed by post hoc multiple comparison (Pairwise) test was used to compare several samples. The significance level was set at $p<0.05$. For bulk carbon isotopes, we used the mixing model proposed by Rasmussen (2010) to estimate the proportion of terrestrial consumption (leaf litter) versus microalgae consumption by both macroinvertebrates. This author established linear relationships between δ^{13}C signatures of river biota, (benthic algae, periphyton, herbivores, gatherers and shredders) along river gradients that allow calculation of the contribution of terrestrial food sources (P_t) to macroinvertebrate functional groups. We used the following equation to estimate the proportion of leaf litter consumed based on the proportion of biofilm microalgae consumed.

$$Pt = (1 - Pa)\ and\ Pa = \frac{(Yc - f) - Yt}{Ya - Yt}$$

Y_a is the measured δ^{13}C signature of the biofilms in each mesocosm; Y_t is the mean measured δ^{13}C signatures of the leaf litters; Y_c represents the δ^{13}C signature of both macroinvertebrates in each mesocosm; *Pt* and *Pa* represent the mixing proportions of allochthonous and autochthonous inputs to macroinvertebrates; *f* is the trophic signature shift relative to algae estimated for stream invertebrates by Rasmussen (2010) using its gradient model.

Concerning total FA, NLFA, and PLFA, the similarities between each basal source and the two macroinvertebrates were analyzed using a Hierarchical Principal Component Classification (Husson et al., 2010). The hierarchical clustering performed on the principal components of the PCA was based on the mean δ^{13}C values of all FA and sterols using Euclidean distances.

Results

Environmental conditions

Temperatures remained stable during the whole experiment with an amplitude of less than 0.5°C between flumes exposed to light (LC: 13.90 ± 1.87°C) and those kept in the dark (DC: 13.46 ± 1.54°C; Supporting information 1). The average amount of light cast on the bottom of the flumes at solar noon (illuminance) were 46 and 2,163 lux in the dark and light conditions, respectively. Thus, darkness was not complete in the dark condition with the conservation of an attenuated Light–Dark cycle.

Macroinvertebrate performances: Survival, emergence and growth

After the 20 days of exposure, survival rates of *G. pulex* were close to 50% and were similar in the two tested conditions (Table 1), whereas survival of *R. semicolorata* nymphs was significantly higher in the light (by 53%; prop-test $p<0.01$). Growth rates of macroinvertebrates were significantly enhanced when reared in the light, by 60% for *G. pulex* (Student t-test $p<0.001$) and by 400 % for *R. semicolorata* ($p<0.01$; Table 1). Emergence rates of *R. semicolorata* subimagos were also significantly higher (by 91%; prop-test $p<0.05$).

Food sources: Leaf litter decomposition and biofilm development

Alder decomposition rates were unaffected by light condition and remaining leaf litter after 20 days was about 25% of the initial mass (Table 2). Total biofilms biovolumes developed on tiles were stable during the experiment (similar at T0 and T20: *see supporting information 2*) and systematically higher in the light compared to dark condition ($p<0.001$-Student t-test; Table 2). A strong biofilm development was observed at T20 on flume walls only in the light, representing 330 x 10^6 ± 103 x 10^6 $\mu m^3.cm^{-2}$ with diatoms accounting for only 31% and chlorophytes being dominant (62%). On the light-exposed tiles the community was largely dominated by diatom species (585 x10^6 ± 274 x10^6 $\mu m^3 cm^{-2}$) accounting for 89% of the total biovolume, with other taxa

being chlorophytes and cyanobacteria (Table 2). In the dark, very few diatoms were enumerated in the tile biofilms and their mean biovolumes were only about 2% of those observed in the light ($12 \pm 8 \times 10^6$ $\mu m^3 . cm^{-2}$).

Gut contents of macroinvertebrates

CPOM and FPOM (Figure 1) were the main items found in *G. pulex* and *R. semicolorata* gut contents (representing more than 80%), followed by diatoms. In the gut contents of *G. pulex* and *R. semicolorata* reared in the light, diatoms were significantly more represented to the detriment of CPOM (about - 65% and - 40% for CPOM, 0.5 to 10% and 0.5 to 20% for diatoms, respectively; Figure 1). For the diet of *G. pulex*, significantly higher FPOM and filamentous algae were also observed in the light (33 and 3.60 %, respectively), revealing a change in feeding habits (from shredder to collector – grazer, see Felten et al., 2008). *R. semicolorata* ingested significantly more CPOM in the dark than in the light (prop test $p<0.01$). Finally, animal preys were found only in *G. pulex*.

Bulk stable isotope analysis and basal source assimilation

In both treatments and at each sampling date (T0 and T20), the isotope signatures of leaf litter (Figure 2) were similar (mean $\delta^{13}C$: -30 ± 0.8 ‰ and $\delta^{15}N$ values < 0; $p = 0.51$ and $p = 0.78$ respectively). Compared to leaf litter, the biofilms were enriched in both isotopes and their signatures differed depending on the conditions tested. Temporally stable $\delta^{13}C$ of -28‰ to -27.9‰ and $\delta^{15}N$ of 2 ± 0.6‰ were registered in the dark whereas in the light, $\delta^{13}C$ signatures reached -20.95 ± 0.4‰ at T20 (Figure 2). $\delta^{13}C$ values recorded in the wall biofilm (T20) were much higher (-14.14 ± 0.6‰). At T20, FPOM showed $\delta^{13}C$ values (-29.01 ± 0.1 ‰) similar to those of leaf litter and biofilm in the dark and intermediate between leaf litter and biofilm in the light (-25.30 ± 2.3‰). Just before the macroinvertebrates were placed in the flumes (T0), they had similar $\delta^{13}C$ values (-25.9 ± 1.3‰) but significant differences in $\delta^{15}N$ values ($p<0.001$) (*G. pulex*: 6.0 ± 0.2‰; *R. semicolorata*: 3.7 ± 0.3‰; Figure 2). At T20, $\delta^{13}C$ and $\delta^{15}N$ signatures did not differ significantly between the two species in the dark ($\delta^{15}N$: 4.02 ± 0.8‰ *vs* 3.84 ± 0.4 ‰, $p=0.8$; $\delta^{13}C$: -26.31 ± 0.3‰ *vs* 26.4 ± 0.2‰, $p=0.7$). In the light, the $\delta^{13}C$ values of *R. semicolorata* were sharply enriched (-16.30 ± 0.6‰, close to the wall biofilm $\delta^{13}C$ signatures,

while δ^{15}N values remained unchanged throughout the survey (about 4‰). *G. pulex* were depleted in δ^{13}C compared to *R. semicolorata* (-23.2 ± 0.9‰), but enriched compared to *G. pulex* in the dark (-26.31 ± 0.3‰). Finally, *G. pulex* δ^{15}N signature decreased from 6.0 ± 0.2‰ (T0) to 4.3 ± 0.6‰ (T20) (Figure 2).

In the light, *Pt* estimates for *R. semicolorata* indicate a very small contribution of alder leaves to the assimilated carbon (Table 3). The proportion of assimilated litter does not exceed 11% (Pt_2 =0.11) and was insignificant (Pt_1 = 0.00) when calculated relative to tile biofilm δ^{13}C signatures. In contrast, *G. pulex* assimilated more carbon from alder leaves with Pt_1 = 0.22 and Pt_2 = 0.56 depending if the calculation considers tile or wall biofilm signatures (Table 3). In the dark the model cannot discriminate between the two food sources (Table 3), end-member signatures being insufficiently differentiated (less than 3‰, see Rasmussen 2010). In this particular case, most of the carbon can be considered to come directly from the litter or its fragmentation in FPOM.

Changes in macroinvertebrate FA amounts and hierarchical clustering of FA mean δ^{13}C values.

Throughout the experiment, no significant changes were observed in the total concentrations of *G. pulex* NLFA and PLFA or between the two treatments (Figure 3). In contrast, *R. semicolorata* nymphs showed similar total PLFA concentrations over time and in both treatments but accumulated significantly higher amounts of NLFA (99.75 ± 11.6 *vs* 24.3 ± 1.99 µg.mg DM^{-1}, ANOVA p<0.05) when reared in the light. This higher storage of NLFA was related to a significantly greater accumulation of saturated fatty acids (SFA), Mono-unsaturated fatty acids (MUFA) and PUFA (Figure 3), a feature not observed in nymphs reared in the dark. In *G. pulex* the amounts of SFA, MUFA, and PUFA remained fairly constant between treatments, except for the significantly higher amount of PUFA in *G. pulex* NLFA under light conditions (15.64 ± 2.67 µg.mg^{-1} DM) compared to dark conditions (6.78 ± 2.70 µg.mg^{-1} DM) (ANOVA p<0.05). These higher concentrations of PUFA in both species were related to the significantly higher PUFA concentrations observed in basal food sources sampled in the light (see Table 2), i.e. wall and tile biofilms (p<0.001) and to a lesser extent FPOM (p<0.01). Hierarchical Clustering on Principal

384 Components performed on the average $\delta^{13}C$ values of all the FAs and sterols detected made it
385 possible to relate the two macroinvertebrate lipid class to the basal sources (Figure 4). For dark
386 conditions, 4 clusters were identified: i) cluster II grouped *G. pulex* isotope signatures (NLFA,
387 PLFA and sterols) with FPOM signatures, ii) cluster III grouped *R. semicolorata* NLFA and PLFA
388 isotope signatures with tile biofilm signatures, while iii) cluster I contained only leaf litter, and iv)
389 cluster IV only contained *R. semicolorata* sterols (Figure 4). In the light, five clusters were
390 identified (Figure 4) : i) cluster IV grouped isotope signatures of *R. semicolorata* NLFA and PLFA
391 with tile biofilm signature, ii) cluster V grouped isotope signatures of *R. semicolorata* sterols with
392 the wall biofilm signature, iii) cluster II grouped *G. pulex* sterol signatures with FPOM signatures,
393 iv) cluster III grouped isotope signatures of *G. pulex* NLFA and PLFA (note that clusters II and III
394 were connected at higher Euclidian distances), while v) cluster I contained only leaf litter (Figure
395 4).
396
397 *Differences in isotopic signatures of FAs*
398 The complete list and details of FAs detected in lipids from basal sources and
399 macroinvertebrates are available as Supporting Information 3 and 4 with the tables S1 (basal
400 sources), S2 (*R. semicolorata*), and S3 (*G. pulex*). In addition, all the available $\delta^{13}C$ values of FAs
401 are listed as additional information (Tables S4 to S5). To better illustrate the effect of the two
402 conditions tested on the origin and transfer of FAs, we focused on the $\delta^{13}C$ signatures of several
403 FAs of interest: i) on abundant 16:0 and 18:1ω9; ii) on selected diatom markers (exclusive:
404 16:2ω4 and 16:4ω1; non-exclusive but overabundant: 16:1ω7; iii) and on essential PUFAs
405 (18:3ω3, 18:2ω6) and LC-PUFAs (ARA: 20:4ω6, EPA:20:5ω3) (see Table 4).
406 In the light, all FA $\delta^{13}C$ values were depleted in leaf litter (-33.47‰ to -29.19‰), with the
407 exception of ARA (-26.82‰) which was more enriched in ^{13}C (Table 4). In line with bulk $\delta^{13}C$
408 signatures, FA $\delta^{13}C$ signatures were highly enriched in tile and wall biofilms (-23.22‰ to -
409 17.46‰) and the ^{13}C enrichment was significant compared to leaf litter FAs (ANOVA $p<0.05$). In
410 contrast, no statistical difference was found in the FA $\delta^{13}C$ signatures between the two biofilms
411 (Table 4). FA signatures in FPOM tended to be intermediate between, typically a 18:2ω6 $\delta^{13}C$
412 value identical to the litter's 18:2ω6 and an EPA $\delta^{13}C$ value identical to those in the biofilms. $\delta^{13}C$

values in *Rhithrogena* were markedly enriched in ^{13}C (-23.64 ‰ to -19.55 ‰) and significantly higher than those in gammarids (-30.51‰ to -24.53 ‰) (ANOVA $p<0.05$), except for 16:4ω1 and EPA (Table 4). We found no statistical difference between the ^{13}C values of 18:1ω9, 18:2ω6, ARA, 18:3ω3 and EPA in *Rhithrogena* NLFA and PLFA and both biofilms (ANOVA $p>0.05$). In *G. pulex*, the ^{13}C contents of 18:2ω6 and ARA were similar to those in litter and FPOM except for ARA from PLFA which was ^{13}C depleted (-28.62 ± 0.10 ‰). 18:3ω3 and EPA $\delta^{13}C$ values in G. pulex were similar to those in FPOM (ANOVA $p>0.05$). Finally, similar trends were observed for 16:0, 16:1ω7 and 18:1ω9, with close values of ^{13}C for *G. pulex* and FPOM, and for *Rhithrogena* and biofilms. Conversely, 16:4ω1 was significantly depleted in ^{13}C in both macroinvertebrates (-22.56 ‰ to -22.37 ‰), compared to the two biofilms (-19.43 ‰ to -17.46 ‰). This was also the case for 16:2ω4, except for *Rhithrogena* NLFA, where the observed difference with the tile biofilm was not significant.

In the dark, there was little contrast in FA $\delta^{13}C$ values between basal sources (Table 4). Leaf litter tended to have the most depleted values, but only 16:0 and 18:3ω3 $\delta^{13}C$ values were significantly enriched in tile biofilm (-28.64 ‰; -30.27 ‰.) compared to litter (-33.58 ‰; -33.80 ‰) (ANOVA $p<0.05$). FA $\delta^{13}C$ signatures in FPOM were identical to those in tile biofilm except for EPA. Overall, FA $\delta^{13}C$ signatures of *G. pulex* and *R. semicolorata* NLFA and PLFA differed little (Table 4). Identical $\delta^{13}C$ values were found for 16:1ω7 18:1ω9 and 18:2ω6, except in *G. pulex* NLFA where 18:2ω6 had a more depleted value (-32.94 ± 0.44‰; ANOVA $p<0.05$).16:0 exhibited similar $\delta^{13}C$ values for both macroinvertebrate and FPOM and 18:3ω3 $\delta^{13}C$ values in *Rhithrogena* were not significantly different than those in basal sources (Table 4). More depleted than in *Rhithrogena*, 18:3ω3 $\delta^{13}C$ values in *Gammarus* NLFA (-35.71 ± 0.25 ‰) and PLFA (-33.21 ± 1.07 ‰) were similar to those of litter (ANOVA $p>0.05$). EPA ^{13}C contents in *G. pulex* (-30.44 ‰ to -29.77 ‰) were depleted compared to *R. semicolorata* (-28.63 ‰ to -27.36 ‰) (ANOVA $p<0.05$) but similar to the values in tile biofilm. In both species, EPA $\delta^{13}C$ values in NLFA and PLFA were enriched (from +3.8‰ to +5.2‰) compared to their respective 18:3ω3 values. No significant difference was found in ARA ^{13}C signatures for the two macroinvertebrates (ANOVA $p>0.05$).

Differences in isotopic signatures of the main sterols

The complete list of sterols detected in the samples and their $\delta^{13}C$ signatures are available as supporting information 5 with Tables S6 and S7. Due to low amounts of phytosterols detected in macroinvertebrates, reliable isotope fractionation values were only obtained for campesterol, β-sitosterol and cholesterol in both species, values that are reported in table 4.

In the dark, isotopic signatures of β-sitosterol were similar in all basal sources (-30.86 ‰ to -30.36 ‰) but significantly depleted in *G. pulex* (-31.58 ± 0.65 ‰; ANOVA $p<0.05$) and probably in *R semicolorata* (only one value: -31.39 ‰). The campesterol in *G. pulex* had a $\delta^{13}C$ value close to that found in biofilm which was more enriched (ANOVA $p<0.05$) than that in litter and FPOM (Table 4). The $\delta^{13}C$ value for cholesterol was significantly higher in biofilm (-27.48 ± 0.33‰; ANOVA $p<0.05$) than in litter and FPOM, and the $\delta^{13}C$ values in *G. pulex* and *R semicolorata* were intermediate (-29.86 ‰ to -30.38 ‰). In the light, the sterol $\delta^{13}C$ values were markedly enriched in biofilms (table 4), especially in the wall biofilm (-23.6 7‰ to -19.0 ‰). The ^{13}C content of sterols in FPOM and litter was similar (-33.77 ‰ to -27.29 ‰) and significantly depleted compared to biofilms (ANOVA $p<0.05$). As observed for FAs, $\delta^{13}C$ values in *Rhithrogena* sterols were enriched (-23.81‰ to -22.86 ‰) and similar to those in both biofilms for cholesterol (-23.43 ±1.4 ‰) and campesterol, but only to tile biofilm for β-sitosterol (table 4). In gammarids, the $\delta^{13}C$ value for cholesterol (-29.31 ± 0.80 ‰) was significantly more depleted than in *Rhithrogena* and intermediate between cholesterol signatures in biofilms and those in litter and FPOM. *G. pulex* $\delta^{13}C$ values of campesterol and β-sitosterol were more depleted than in *Rhithrogena*.

Discussion

Our study highlights the importance that different sources of organic matter may have on the development of macroinvertebrates from different FFG.

Bulk stable- isotope signatures and origin of the assimilated carbon

In light conditions, *Rhithrogena* nymphs and *Gammarus* had access to an important source of autochthonous organic matter. Similar to results recently observed for another Heptageniidae species, *Ecdyonurus* sp. (Kühmayer et al., 2020), most of *Rhithrogena*'s carbon

was derived from autochthonous organic matter (tile and wall biofilm) as estimated by the mixing model and *Rhithrogena*'s ^{13}C-enriched signatures. *Gammarus pulex* derived between 22% and 56% of its carbon from terrestrial sources, primarily FPOM (based on their gut contents and results from the Hierarchical Clustering model). This percentage of allochthonous food in the gammarid isotope signatures was lower than expected, but must be related to the plasticity of their feeding behavior (Felten et al., 2008). In dark conditions and despite having distant biological traits, *Rhithrogena* nymphs and *Gammarus* had the same trophic positions and similar stable carbon isotope compositions. Assimilated carbon was of detrital origin, likely from fine particles derived from litter fragmentation (FPOM), and from biofilm. This biofilm was predominantly heterotrophic, although a few diatoms may have remained, explaining the slight enrichment in ^{13}C compared to FPOM (Risse-Buhl et al., 2012).

Influence of food sources and their PUFA levels on the growth of both species

The absence of well-developed autotrophic biofilms affected the performance of our two macroinvertebrates reared in the dark, in particular the *Rhithrogena* nymphs. In streams, the quality of the food resources can be as limiting as their availability to consumers (Florès et al., 2014) and quality depends on the presence of autochthonous primary production (Torres-Ruiz et al., 2007; Guo et al., 2016b). The content of essential lipid compounds in biofilm microalgae has the greatest influence on nutritional quality (Crenier et al., 2017; Twining et al., 2017; Guo et al., 2018; Torres-Ruiz & Wehr, 2019). In freshwater, essential life history traits such as growth rate, fecundity rate and survival of many invertebrates seem to depend on the nutritional supply of essential PUFAs (Ruess & Müller-Navarra, 2019) and/or phytosterols that can be bioconverted into cholesterol (Martin-Creuzburg & Merkel, 2016). Furthermore, we show that access to these lipids from autotrophic biofilms has impacted some of the life history traits of our two species. When *Rhithrogena* nymphs had access to autotrophic biofilms, all aspects of their performance (survival and emergence rates, growth parameters) were significantly higher than those of their congeners reared in the dark. Although PLFA levels did not differ between nymphs from the two treatments, mayflies reared in the light accumulated huge amounts of NLFA (99.75 ± 11.6 $\mu g.mg^{-1}$ DM). Knowing that in insects most of the NLFA are in the form of triacylglycerols (TAG) (Arrese

499 & Soulages, 2010) this represents approximately 112 µmol.g^{-1} DM of TAG. Such concentrations
500 are among the highest observed in late instar of *R. semicolorata* nymphs from mountain streams
501 (mean: 60 µmol.g^{-1} DM; max: 118 µmol.g^{-1} DM; see in Winkelmann & Koop, 2007). In contrast,
502 dark-reared nymphs contained only 24.30 ± 2.0 µg.mg^{-1} DM of NLFA, representing approximately
503 27.5 µmol.g^{-1} DM of TAG, consistent with the lowest values reported by Winkelmann & Koop
504 (2007). We found that the mean δ^{13}C signature of the FA pool in *Rhithrogena* NLFA was indeed
505 derived from biofilms which is in line with Kühmayer et al. (2020), who reported that *Ecdyonurus*
506 sp. acquired its FAs primarily from microalgae. During the last weeks before emergence, energy
507 obtained from food is used to maximize growth with the remainder is stored as TAG and glycogen
508 or used for egg maturation by female *Rhithrogena semicolorata* nymphs (Canavoso et al., 2001;
509 Winkelmann & Koop, 2007). Thus, the amount of lipids stored is intended to cover energy needs
510 during the mating period and depends largely on the quantity and quality of available food
511 sources (Winkelmann & Koop, 2007). While the nymphs certainly fulfilled their FA requirements in
512 the presence of autotrophic biofilms, the lipid and nutritional needs of dark-reared nymphs were
513 certainly not met. In the dark, *Rhithrogena* derived most of their NLFAs from detrital biofilm and it
514 is likely that they ingested large amounts of detrital particles to compensate for the absence of
515 microalgae. Such compensatory feeding behaviour has already been observed in caddisfly larvae
516 facing poor quality food (Florès et al., 2014).

517 Regarding gammarids, access to autotrophic biofilms allowed a significantly higher growth
518 when reared in the light. In crustaceans, growth depends on the nutritional supply of lipid
519 compounds, such as LC-PUFAs (Müller-Navarra et al., 2000; Aguilar et al., 2012) or cholesterol
520 precursor Δ5-sterols (Gergs et al., 2015). Results from the hierarchical clustering indicated that
521 NLFA were mainly derived from FPOM in *G. pulex* under both light and dark conditions. The lack
522 of effect on their survival rates and NLFA concentrations is related to their ability to meet their
523 basic metabolic needs by ingesting leaf debris from good quality litter such as alder leaves (Little
524 & Altermatt, 2019). However, we suggest that only the occurrence of microalgae colonizing
525 FPOM can explain the better growth rate observed in light-reared *G. pulex*. In this sense, Crenier
526 et al. (2017) proved that diatoms associated with leaf litter were essential for *Gammarus*
527 *fossarum* growth.

528

529 ***Origin of FAs and essential PUFAs according to the conditions tested***

530 CSIA allowed us to establish the origin of the essential PUFAs as well as the main sterols
531 detected. In *Rhithrogena* reared in the light, the high ^{13}C-enrichments observed in PUFAs, 16:0,
532 18:1ω9 and diatom markers (16:1ω7, 16:4ω1) resembled those observed in the autotrophic
533 biofilms. Undoubtedly, the enriched δ^{13}C values of EPA and 18:3ω3 in the nymphs NL indicate
534 that such essential FAs originated from biofilms. We suggest that EPA in *Rhithrogena* was
535 directly derived from diatoms in tile biofilms and 18:3ω3 came from microalgae in the wall biofilm.
536 The same applies for ω6 PUFAs and other FAs highly enriched in ^{13}C detected in *R.*
537 *semicolorata*. FAs in *G. pulex* reared in the light may have more diverse origins. As observed in
538 *Rhithrogena,* 16:4ω1 was incorporated from diatoms in both types of biofilms with only slight
539 depletion. This confirms that microalgae were indeed assimilated by *G. pulex*. However, with δ^{13}C
540 signatures between -30.50 ‰ and - 29.50 ‰ in *G. pulex*, 18:2ω6 could not originate from biofilms
541 so must have come from ingested FPOM. In *G. pulex* ARA and EPA were depleted in ^{13}C relative
542 to FPOM and enriched relative to their respective precursors (18:2ω6 and 18:3ω3), so these LC-
543 PUFA signatures were likely modified by lipid metabolic activity. Under dark conditions,
544 differences in FA δ^{13}C values among basal sources did not exceed 2.7‰, confirming the near-
545 absence of ^{13}C-enriched microalgae. In *Gammarus* and *Rhithrogena*, 18:3ω3 and 18:2ω6 from
546 both lipid classes were exclusively of detrital origin. The constraint imposed by the lack of
547 microalgae acted on ARA and EPA levels in both species, which were significantly lower in the
548 dark. We think that ARA originated from the bioconversion of 18:2ω6 as did EPA from 18:3ω3.
549 Both PUFAs were indeed enriched in ^{13}C relative to their precursors, which is consistent with an
550 input of heavy carbon atoms during 18:2ω6 and 18:3ω3 elongation process (Hayes, 2001;
551 Gladyshev et al., 2012).

552

553 ***Role of microalgae in meeting the LC-PUFAs and sterols requirements of both***
554 ***species***

555 In our opinion, the need to synthesize 20:4ω6 and 20:5ω3 is likely the main reason for
556 the poorer performance observed in both species under dark conditions. Indeed, experiments

examining penaeid shrimp development reported that both dietary PUFAs were important to their survival and development (Merican & Shim, 1996). Growth was generally better when combinations of ARA and EPA were provided in their diet, limiting their energy-intensive synthesis (Glencross et al., 2002). In addition, dietary EPA or ARA are known to improves the reproductive performance of several crustacean species (Schlotz et al., 2013; Ginjupalli, et al., 2015). Sterol deficiency may also have serious consequences for the life cycle of gammarids (Gergs et al., 2015) and most likely also for aquatic insects, based on observations made on terrestrial species (Behmer, 2017). Under day light conditions, the isotopic signatures of dietary campesterol and β-sitosterol detected in both species were unequivocal. Those highly enriched in ^{13}C were derived from biofilm microalgae in *Rhithrogena,* while those depleted in ^{13}C originated from FPOM in *G pulex*. Low levels of cholesterol were detected in autotrophic biofilms and we do not know whether this was sufficient to cover the needs of *Rhithrogena*. The isotopic signatures being close, the possibility that a substantial part of mayfly cholesterol came from microalgae cannot be ignored, since this sterol can be abundant in certain benthic diatom species (Jaramillo-Madrid et al., 2019). However, the occurrence of its immediate precursor (desmosterol) in *Rhithrogena* may suggest that cholesterol synthesis from dietary sterols also occurred. We also think that *Gammarus* has instead dealkylated dietary β-sitosterol to produce cholesterol. The depleted signature of its residual β-sitosterol and its enriched ^{13}C cholesterol seem to point to this (Hayes, 2001). In the dark, the high abundance of β-sitosterol in detrital resources makes it the probable precursor of cholesterol synthesis in both macroinvertebrates where desmosterol was also detected. However, with access to alder leaf fragments, it is likely that sterol nutritional constraints were limited for both species. Indeed, campesterol and β-sitosterol belong to $\Delta 5$ phytosterols that are readily dealkylated by arthropods (Martin-Creuzburg et al., 2014; Behmer, 2017). Under light conditions, the ability to produce cholesterol by some benthic diatoms definitely adds to the nutritional value of autotrophic biofilms.

Conclusion

Our study clearly indicated that autochthonous food sources were important in meeting the biochemical requirements for LC-PUFAs of both macroinvertebrate species in early summer,

586 leading to higher rates of growth (*G. pulex* and *R. semicolorata*) and emergence (*R.*
587 *semicolorata*). In their last instars, *Rhithrogena* are highly dependent on biofilm microalgae from
588 which they derive most of their carbon, in addition to essential FAs such as ARA and EPA and
589 some dietary cholesterol. Limitation of LC-PUFAs appears to be a major ecological constraint for
590 grazing Heptageniidae in headwater streams when feeding solely on leaf detrital particles
591 because epilithic biofilms are limited by shading. For *G. pulex*, our experiment showed that
592 detrital food sources remain quantitatively important in terms of supply of carbon and sterols. This
593 might be even more important when fine particles come from tree species known for the
594 palatability of their leaf litter (Little & Altermatt, 2019). Microalgae collected in biofilm and/or with
595 FPOM may have usually been considered as a minor complementary food but here they appear
596 to be of paramount nutritional importance to meet a large part of the LC PUFA needs of
597 amphipods. This also emphasizes the importance of fine particles of organic matter, and their
598 exact composition in allochthonous detrital fragments and autochthonous photosynthetic material
599 should be investigated in greater detail in headwater streams as well as their relative contribution
600 to food webs.
601
602

603 ## Acknowledgment

604 We thank the CNSS (Conservatoire National du Saumon Sauvage, Chanteuges, France)
605 for the provision of the reach and daily technical assistance. We also thank Ms. Frances Van Wyk
606 de Vries for the improvement of the English text. This project was funded by EC2CO (INSU-
607 CNRS) IFODPSYLO 2018-2020.
608

609 ## Author contribution statement

610 Conceptualisation: CD, MD, AB. Developing methods: TLV, CD, MD, VF, AB. Conducting the
611 research: TLV, CD, VF, MD, ML, MC. Data analysis: TLV, CD, MD, VF. Preparation of figures
612 and tables: TLV, CD. Data interpretation and writing: TLV, CD, MD, VF, AB, ML, MC.
613

Data availability statement

Data are available from authors upon reasonable request.

Conflict of interest

The authors have no conflict of interest to declare.

References

Aguilar, V., Racotta, I. S., Goytortúa, E., Wille, M., Sorgeloos, P., Civera, R., & Palacios, E. (2012). The influence of dietary arachidonic acid on the immune response and performance of Pacific whiteleg shrimp, Litopenaeus vannamei, at high stocking density. *Aquac. Nutr.,* 18: 258–271.

Ahlgren, G., Vrede, T., & Goedkoop, W. (2009). Fatty acid ratios in freshwater fish, zooplankton and zoobenthos–are there specific optima?. Lipids in aquatic ecosystems, Springer, pp. 147–178.

Alberts, J. M., Fritz, K. M., & Buffam, I. (2018). Response to basal resources by stream macroinvertebrates is shaped by watershed urbanization, riparian canopy cover, and season. *Freshw. Sci.*, 37: 640–652.

Allan, J. D., & Castillo, M. M. (2007). Stream ecology: structure and function of running waters. Springer Science & Business Media.

Arrese, E. L., & Soulages, J. L. (2010). Insect fat body: energy, metabolism, and regulation. *Annu. Rev. Entomol.*, 55: 207–225.

Behmer, S. T. (2017). Overturning dogma: tolerance of insects to mixed-sterol diets is not universal. *Curr. Opin. Insect Sci.*, 23: 89–95.

642 Brett, M. T., Bunn, S. E., Chandra, S., Galloway, A. W. E., Guo, F., Kainz, M. J., … Wehr, J. D.
643 (2017). How important are terrestrial organic carbon inputs for secondary production in
644 freshwater ecosystems?. *Freshw. Biol.*, 62: 833–853.
645 Caroll, T. M., Thorp, J. H., & Roach, K. A. (2016). Autochthony in karst spring food webs.
646 *Hydrobiologia*, 776: 173-191.
647 Canavoso, L. E., Jouni, Z. E., Karnas, K. J., Pennington, J. E., & Wells, M. A. (2001). Fat
648 metabolism in insects. *Annu. Rev. Nutr.*, 21: 23–46.
649 Cashman, M. J., Wehr, J. D., & Truhn, K. (2013). Elevated light and nutrients alter the nutritional
650 quality of stream periphyton. *Freshw. Biol.*, 58: 1447–1457.
651 Collins, S. M., Kohler, T. J., Thomas, S. A., Fetzer, W. W., & Flecker, A. S. (2016). The
652 importance of terrestrial subsidies in stream food webs varies along a stream size gradient.
653 *Oikos*, 125: 674–685.
654 Crenier, C., Arce-Funck, J., Bec, A., Billoir, E., Perrière, F., Leflaive, J., … Danger, M. (2017).
655 Minor food sources can play a major role in secondary production in detritus-based
656 ecosystems. *Freshw. Biol.*, 62: 1155–1167.
657 Felten, V., Tixier, G., Guérold, F., De Crespin De Billy, V., & Dangles, O. (2008). Quantification of
658 diet variability in a stream amphipod: Implications for ecosystem functioning. *Fundam. Appl.*
659 *Limnol.*, 170: 303–313.
660 Florès, L., Larrañaga, A., & Elosegi, A. (2014). Compensatory feeding of a stream detritivore
661 alleviates the effects of poor food quality when enough food is supplied. *Freshw. Sci.*, 33:
662 134–141.
663 Gergs, R., Steinberger, N., Beck, B., Basen, T., Yohannes, E., Schulz, R., & Martin-Creuzburg, D.
664 (2015). Compound-specific $\delta^{13}C$ analyses reveal sterol metabolic constraints in an aquatic
665 invertebrate. *Rapid Commun. Mass Spectrom.*, 29: 1789–1794.
666 Ginjupalli, G. K., Gerard, P. D., & Baldwin, W. S. (2015). Arachidonic acid enhances reproduction
667 in *Daphnia magna* and mitigates changes in sex ratios induced by pyriproxyfen. *Environ.*
668 *Toxicol. Chem.*, 34: 527–535.
669 Gladyshev, M. I., Sushchik, N. N., Kalachova, G. S., & Makhutova, O. N. (2012). Stable isotope
670 composition of fatty acids in organisms of different trophic levels in the Yenisei River. *PLoS*

671 *One*, 7: e34059.
672 Glencross, B. D., Smith, D. M., Thomas, M. R., & Williams, K. C. (2002). The effect of dietary n-3
673 and n-6 fatty acid balance on the growth of the prawn Penaeus monodon. *Aquac. Nutr.*, 8:
674 43–51.
675 Guo, F., Bunn, S. E., Brett, M. T., Fry, B., Hager, H., Ouyang, X., & Kainz, M. J. (2018). Feeding
676 strategies for the acquisition of high-quality food sources in stream macroinvertebrates:
677 Collecting, integrating, and mixed feeding. *Limnol. Oceanogr.*, 63: 1964–1978.
678 Guo, F., Kainz, M. J., Valdez, D., Sheldon, F., & Bunn, S. E. (2016a). High-quality algae attached
679 to leaf litter boost invertebrate shredder growth. *Freshw. Sci.*, 35: 1213–1221.
680 Guo, F., Kainz, M. J., Sheldon, F., & Bunn, S. E. (2016b). The importance of high-quality algal
681 food sources in stream food webs–current status and future perspectives. *Freshw. Biol.*, 61: 815–
682 831.
683 Hayes, J. M. (2001). Fractionation of carbon and hydrogen isotopes in biosynthetic processes.
684 *Rev. Mineral. Geochem.*, 43: 225–277.
685 Honeyfield, D. C., & Maloney, K. O. (2015). Seasonal patterns in stream periphyton fatty acids
686 and community benthic algal composition in six high-quality headwater streams.
687 *Hydrobiologia*, 744: 35–47.
688 Husson, F., Josse, J., & Pagès, J. (2010). Analyse de données avec R - Complémentarité des
689 méthodes d'analyse factorielle et de classification. 42èmes Journées de Statistique, 2010,
690 Marseille, France, inria-00494779: 1-7.
691 Jaramillo-Madrid, A. C., Ashworth, J., Fabris, M., & Ralph, P. J. (2019). Phytosterol biosynthesis
692 and production by diatoms (Bacillariophyceae). *Phytochemistry*, 163: 46–57.
693 Koussoroplis, A. -M., Bec, A., Perga, M. -E., Koutrakis, E., Desvilettes, C., & Bourdier, G. (2010).
694 Nutritional importance of minor dietary sources for leaping grey mullet *Liza saliens*
695 (Mugilidae) during settlement: insights from fatty acid δ^{13}C analysis. *Mar. Ecol. Prog. Ser.*,
696 404: 207–217.
697 Kühmayer, T., Guo, F., Ebm, N., Battin, T. J., Brett, M. T., Bunn, S. E., … Kainz, M. J. (2020).
698 Preferential retention of algal carbon in benthic invertebrates: Stable isotope and fatty acid
699 evidence from an outdoor flume experiment. *Freshw. Biol.*, *65: 1200-1209.*

Little, C. J., & Altermatt, F. (2019). Differential resource consumption in leaf litter mixtures by native and non-native amphipods. *Aquat. Ecol.*, 53: 151–162.

Martin-Creuzburg, D., & Merkel, P. (2016). Sterols of freshwater microalgae: Potential implications for zooplankton nutrition. *J. Plankton Res.*, 38: 865–877.

Martin-Creuzburg, D., Oexle, S., & Wacker, A. (2014). Thresholds for sterol-limited growth of Daphnia magna: a comparative approach using 10 different sterols. *J. Chem. Ecol.*, 40(9):1039.

Merican, Z. O., & Shim, K. F. (1996). Qualitative requirements of essential fatty acids for juvenile *Penaeus monodon*. *Aquaculture*, 147 (3), 275–291.

Rasmussen, J. B. (2010). Estimating terrestrial contribution to stream invertebrates and periphyton using a gradient-based mixing model for δ^{13}C. *J. Anim. Ecol.,* 79: 393–402.

Risse-Buhl, U., Trefzger, N., Seifert, A. -G., Schönborn, W., Gleixner, G., & Küsel, K. (2012). Tracking the autochthonous carbon transfer in stream biofilm food webs. *FEMS Microbiol. Ecol.*, 79: 118–131.

Ruess, L., & Müller-Navarra, D. (2019). Essential biomolecules in food webs. *Front. Ecol. Evol.*, 7: 269.

Schlotz, N., Ebert, D., & Martin-Creuzburg, D. (2013). Dietary supply with polyunsaturated fatty acids and resulting maternal effects influence host–parasite interactions. *BMC Ecol.*, 13: 1–11.

Tank, J. L., Rosi-Marshall, E. J., Griffiths, N. A., Entrekin, S. A., & Stephen, M. L. (2010). A review

of allochthonous organic matter dynamics and metabolism in streams. *J. North. Am. Benthol. Soc*., 29: 118–146.

Tocher, D. R., Betancor, M. B., Sprague, M., Olsen, R. E., & Napier, J. A. (2019). Omega-3 long-chain polyunsaturated fatty acids, EPA and DHA: bridging the gap between supply and demand. *Nutrients*, 11: 89.

Torres-Ruiz, M., & Wehr, J. D. (2019). Complementary information from fatty acid and nutrient stoichiometry data improve stream food web analyses. *Hydrobiologia*, 847: 629–645.

Torres-Ruiz, M., Wehr, J. D., & Perrone, A. A. (2007). Trophic relations in a stream food web:

importance of fatty acids for macroinvertebrate consumers. *J. North. Am. Benthol. Soc.*, 26: 509–522.

Twining, C. W., Josephson, D. C., Kraft, C. E., Brenna, J. T., Lawrence, P., & Flecker, A .S. (2017). Limited seasonal variation in food quality and foodweb structure in an Adirondack stream: Insights from fatty acids. *Freshw. Sci.*, 36: 877–892.

Winkelmann, C., & Koop, J. H. E. (2007). The management of metabolic energy storage during the life cycle of mayflies: a comparative field investigation of the collector-gatherer *Ephemera danica* and the scrapper *Rhithrogena semicolorata*. *J. Comp. Physiol*., 177: 119-128.

Tables

Table 1 Survival rate, emergence rate, final size and daily growth rate of the two macroinvertebrates reared under dark conditions (DC) and light conditions (LC). (Prop.test was used for survival and emergence rates and a Mann-Whitney test for size parameters, *: $p<0.05$; **: $p<0.001$; ***: $p<0.0001$; ns: not significant).

Analysis	Species	T20 - DC mean ± sd	T20 - LC mean ± sd	*p*
Survival rate (%)	*G. pulex*	48.3 ± 12.5	55.7 ± 5.7	ns
	R. semicolorata	36.0 ± 4.9	55.0 ± 1.3	**
Emergence rate (%)	*R. semicolorata*	9.3 ± 0.0	17.8 ± 5.9	*
Sizes (mm) and daily growth rate ($mm.d^{-1}$)	*G. pulex*			
	Total body lenght (TBL)	6.118 ± 0.767	6.739 ± 0.867	***
	Daily growth rate (DGR)	0.010 ± 0.007	0.016 ± 0.008	***
	R. semicolorata			
	Total body lenght (TBL)	7.116 ± 1.068	9.949 ± 1.863	**
	Daily growth rate (DGR)	0.005 ± 0.007	0.025 ± 0.013	**

Table 2 Main characteristics of basal sources sampled at the end of the experiment in dark (DC) and light conditions (LC) including: 1) remaining litter biomass (ash-free dry mass-AFDM) and litter decomposition rates (k) calculated from the start of the survey, 2) the biovolumes of tile biofilm and wall biofilm, 3) the amounts of Saturated Fatty Acid (SFA), Mono-unsaturated Fatty Acids (MUFA) and Polyunsaturated Fatty Acids (PUFA) detected in each basal source. Values are mean ± SD. (Student *t*-test, *: $p<0.05$; **: $p<0.001$; ns: not significant).

Samples	Analysis	T20 - DC	T20 - LC	*p*
Leaf litter	AFDM (mg)	1.40 ± 0.08	1.52 ± 0.17	ns
	Decomposition rate (*k*)	0.030 ± 0.001	0.028 ± 0.003	ns
Tile biofilm	Diatoms (x10^6 µm^3. cm^{-2})	12 ± 8	449 ± 75	**
	Chlorophyta (x10^6 µm^3.cm^{-2})	0	25 ± 28	-
	Cyanobacteria (x10^6 µm^3.cm^{-2})	0	24 ± 21	-
Wall biofilm	Diatoms (x10^6 µm^3.cm^{-2})		104 ± 75	-
	Chlorophyta (x10^6 µm^3.cm^{-2})		206 ± 97	-
	Cyanobacteria (x10^6 µm^3.cm^{-2})		19 ± 23	-
Tile biofilm	SFA (µg.mg^{-1} DM)	4.35 ± 2.23	7.84 ± 0.99	ns
	MUFA (µg.mg^{-1} DM)	1.48 ± 0.78	4.81 ± 0.22	**
	PUFA (µg.mg^{-1} DM)	0.25 ± 0.18	3.24 ± 0.32	***

Table 3 Mixing model estimates (with SE) of allochthonous matter consumption by both macroinvertebrates at T20.

$\delta^{13}C_{MIV}$ (i.e. Y_c) is $\delta^{13}C$ signature in macroinvertebrates ; Y_{a1} and Y_{a2} are the measured $\delta^{13}C$ signatures of tile and wall biofilms respectively ; Y_t is the mean measured $\delta^{13}C$ values of the leaf litter in each treatment ; P_{t1} and P_{t2} represent the proportions of allochthonous sources consumed based on the proportion of tile or wall biofilm consumed ; f is the trophic shift relative to periphyton signatures estimated for stream herbivores / grazers (HERB) or shredders (SHR) by Rasmussen (2010) and f is negative ; NA means model not applicable (see text). DC means dark condition and LC means light conditions.

		$\delta^{13}C$ MIV	P_{t1}	P_{t2}	Y_t	Y_{a1}	Y_{a2}	f values
LC	*Rhithrogena semicolorata*	-16.3 ‰ ± 0.6	0.00 ± 0.13	0.11 ± 0.03	-29.62 ‰	-20.95 ‰ ± 0.4	-14.14 ‰ ± 0.6	$f_{HER/ALG}$: - 0.4
LC	*Gammarus pulex*	-23.2 ‰ ± 0.9	0.22 ± 0.09	0.56 ± 0.06	-29.62 ‰	-20.95 ‰ ± 0.4	-14.14 ‰ ± 0.6	$f_{SHR/ALG}$: - 0.4
DC	*Rhithrogena semicolorata*	-26.4 ‰	*NA*	-	-29.87 ‰	-27.9 ‰ ± 0.1	-	$f_{HER/ALG}$: - 0.4
DC	*Gammarus pulex*	-26.03 ‰ ± 0.3	*NA*	-	-29.87 ‰	-27.9 ‰ ± 0.1	-	$f_{SHR/ALG}$: - 0.4

Table 4 δ^{13}C values of the selected fatty acids and sterols in basal sources and in *G. pulex* and *R. semicolorata* under Light Conditions or Dark Conditions. Significant differences (one-way ANOVA with $p < 0.05$) are indicated by different letters. NLFA: Neutral lipid fatty acids; PLFA: Polar lipid fatty acids.

Dark conditions	Leaf litter	FPOM	Tile biofilm	NLFA R. semicolorata	PLFA R. semicolorata	NLFA G. puLex	PLFA G. pulex
16:0	-33.58 ± 0.01 ^{a}	-30.77 ± 2.04 ^{ab}	-28.64 ± 0.65 ^{b}	-30.64 ± 0.61 ^{ab}	-30.77 ± 2.99 ^{ab}	-30.88 ± 0.26 ^{ab}	-30.91 ± 0.16 ^{ab}
16:1ω7	-29.56 ± 0.30 ^{a}	-28.80 ± 3.95	-30.59 ± 0.49 ^{a}	-29.79 ± 0.09 ^{a}	-30.25 ± 3.08 ^{a}	-30.40 ± 0.25 ^{a}	-30.30 ± 1.01 ^{a}
18:1ω9	-30.85 ± 1.53 ^{ab}	-29.16 ± 1.00 ^{ab}	-27.70 ± 0.13 ^{a}	-30.41 ± 0.11 ^{b}	-30.58 ± 0.77 ^{b}	-29.83 ± 0.08 ^{b}	-30.44 ± 0.05 ^{a}
18:2ω6	-30.99 ± 0.35 ^{a}	-31.14 ± 1.19 ^{a}	-30.79 ± 0.21 ^{a}	-31.15 ± 0.90 ^{a}	-30.75 ± 0.81 ^{a}	-32.94 ± 0.44 ^{b}	-30.53 ± 0.41 ^{a}
18:3ω3	-33.80 ± 0.04 ^{ac}	-29.96	-30.27 ± 3.30 ^{b}	-32.45 ± 0.45 ^{ab}	-32.33 ± 0.54 ^{ab}	-35.71 ± 0.25 ^{c}	-33.21 ± 1.07 ^{ac}
20:4ω6				-29.82 ± 0.67 ^{ab}	-28.89 ± 0.60 ^{a}	-30.64 ± 0.29 ^{b}	-29.83 ± 0.15 ^{ab}
20:5ω3		-24.42	-30.18 ± 0.89 ^{a}	-28.63 ± 0.08 ^{b}	-27.36 ± 0.95 ^{c}	-30.44 ± 0.30 ^{d}	-29.77 ± 0.28 ^{ad}

Light conditions	Leaf litter	FPOM	Tile biofilm	Wall biofilm	NLFA R. semicolorata	PLFA R. semicolorata	NLFA G. pulex	PLFA G. pulex
16:0	-33.47 ± 0.31 ^{a}	-25.71 ± 0.69 ^{b}	-21.81 ± 0.42 ^{b}	-22.08 ± 2.05 ^{b}	-19.76 ± 0.49 ^{d}	-21.70 ± 0.50 ^{c}	-27.39 ± 1.33 ^{be}	-27.75 ± 0.72 ^{e}
16:1ω7	-29.19 ± 0.16 ^{a}	-21.31 ± 1.37 ^{b}	-18.68 ± 0.98 ^{c}	-19.12 ± 2.65 ^{bc}	-19.55 ± 0.16 ^{bc}	-19.57 ± 0.53 ^{bc}	-24.59 ± 0.54 ^{d}	-24.53 ± 0.91 ^{d}
18:1ω9	-30.00 ± 2.06 ^{a}	-25.89 ± 1.25 ^{b}	-23.49 ± 0.56 ^{bc}	-22.72 ± 0.82 ^{c}	-20.96 ± 1.22 ^{c}	-21.56 ± 0.44 ^{c}	-27.60 ± 0.15 ^{b}	-27.75 ± 0.24 ^{b}
16:2ω4	-28.14	-23.25 ± 1.40 ^{a}	-17.92 ± 2.57 ^{a}	-17.72	-21.28 ± 0.19 ^{a}	-23.40 ± 0.71 ^{a}	-24.14 ± 1.17 ^{a}	
16:4ω1			-19.43 ± 1.83 ^{a}	-17.46	-22.37 ± 0.79 ^{b}	-22.47 ± 1.01 ^{b}	-22.56	
18:2ω6	-30.89 ± 0.35 ^{a}	-29.69 ± 5.00 ^{a}	-21.57 ± 2.97 ^{b}	-21.32 ± 3.06 ^{b}	-22.98 ± 0.29 ^{b}	-23.64 ± 0.38 ^{b}	-30.51 ± 1.81 ^{a}	-29.51 ± a
18:3ω3	-33.30 ± 3.96 ^{a}	-25.12 ± 4.45 ^{bd}	-23.22 ± 0.93 ^{bc}	-19.61 ± 1.66 ^{c}	-23.19 ± 0.53 ^{bc}	-23.24 ± 0.30 ^{bc}	-27.77 ± 0.12 ^{d}	-25.99 ± 2.12 ^{bd}
20:4ω6	-26.82	-26.42 ± 2.46 ^{a}	-20.69 ± 0.70 ^{b}		-21.64 ± 0.36 ^{b}	-21.94 ± 0.48 ^{b}	-28.00 ± 0.58 ^{ac}	-28.62 ± 0.10 ^{c}
20:5ω3	-32.70 ± 0.23 ^{a}	-23.56 ± 2.23 ^{bc}	-19.41 ± 1.71 ^{b}	-23.18 ± 3.10 ^{bc}	-22.29 ± 0.28 ^{bc}	-21.92 ± 0.10 ^{bc}	-25.33 ± 0.04 ^{c}	-26.05 ± 0.75 ^{c}

Dark conditions	Leaf litter	FPOM	Tile biofilm	*R. semicolorata*	G. pulex
cholesterol	-34.83 ± 0.11 ^{a}	-34.01 ± 1.24 ^{a}	-27.48 ± 0.33 ^{b}	*-30.38*	*-29.86* ± 0.98 ^{c}
campesterol	-33.03 ± 0.23 ^{a}	-33.16 ± 0.82 ^{a}	-30.21 ± 0.93 ^{b}		*-29.76*
β-sitosterol	-30.36 ± 0.25 ^{a}	-30.62 ± 0.41 ^{ab}	-30.86 ± 0.16 ^{ac}	*-31.39*	*-31.58* ± 0.65 ^{c}

Light conditions	Leaf litter	FPOM	Tile biofilm	Wall biofilm	*R. semicolorata*	G. pulex
cholesterol	*-33.77* ± 0.08 ^{a}	*-32.11* ± 1.56 ^{a}	-25.12 ± 0.72 ^{b}	-23.69 ± 0.63 ^{b}	-23.43 ± 1.40 ^{b}	-29.31 ± 0.80 ^{c}

Figures

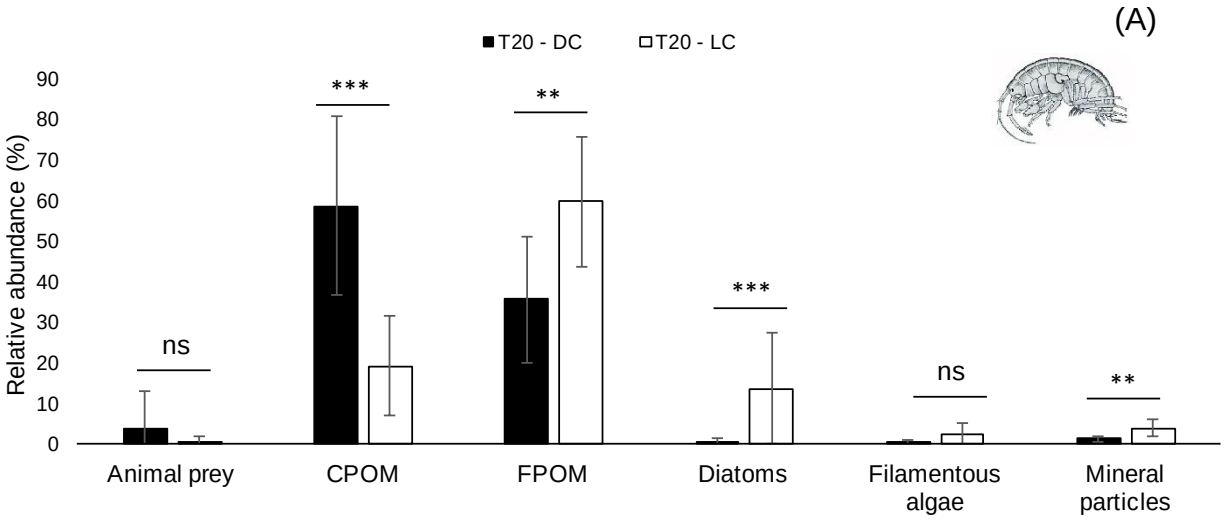
(A)
T20 - DC
T20 - LC
Relative abundance (%)
90
80
70
60
50
40
30
20
10
0
***
**
***
ns
ns
**
Animal prey
CPOM
FPOM
Diatoms
Filamentous algae
Mineral particles

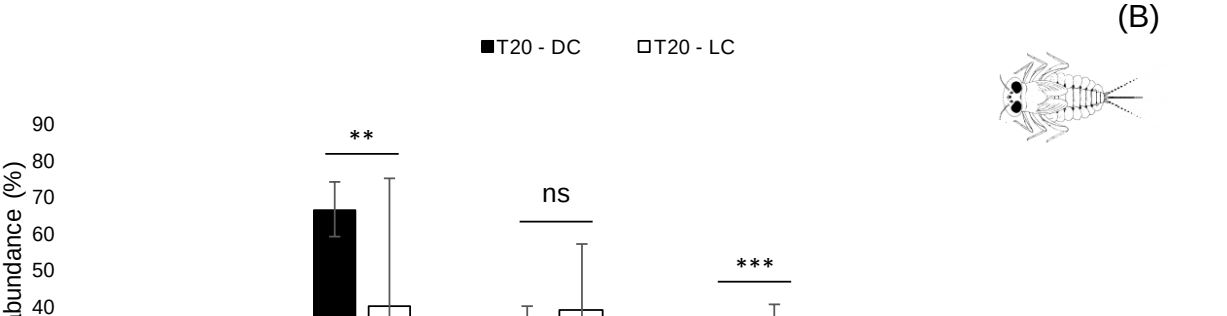
(B)
T20 - DC
T20 - LC
90
80
70
60
50
40
**
ns
***

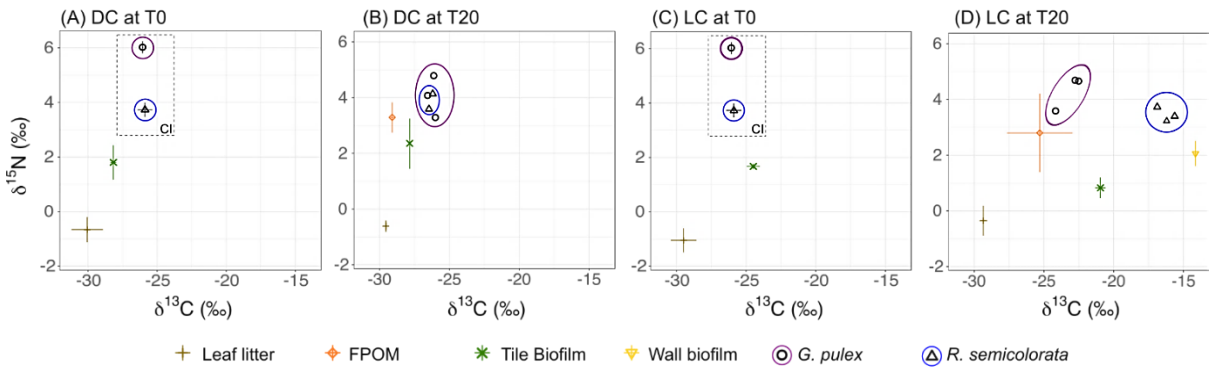

Figure 2 Stable isotope Analysis

δ^{15}N and δ^{13}C biplot showing the basal sources (mean ± SD) and individual values of *G. pulex* (orange circles) and *R. semicolorata* (blue circles) in dark conditions at T0 (A) and T20 (B) and in light conditions at T0 (C) and T20 (D). Collected individuals (CI) at T0 are shown for information in the box with a dotted line.

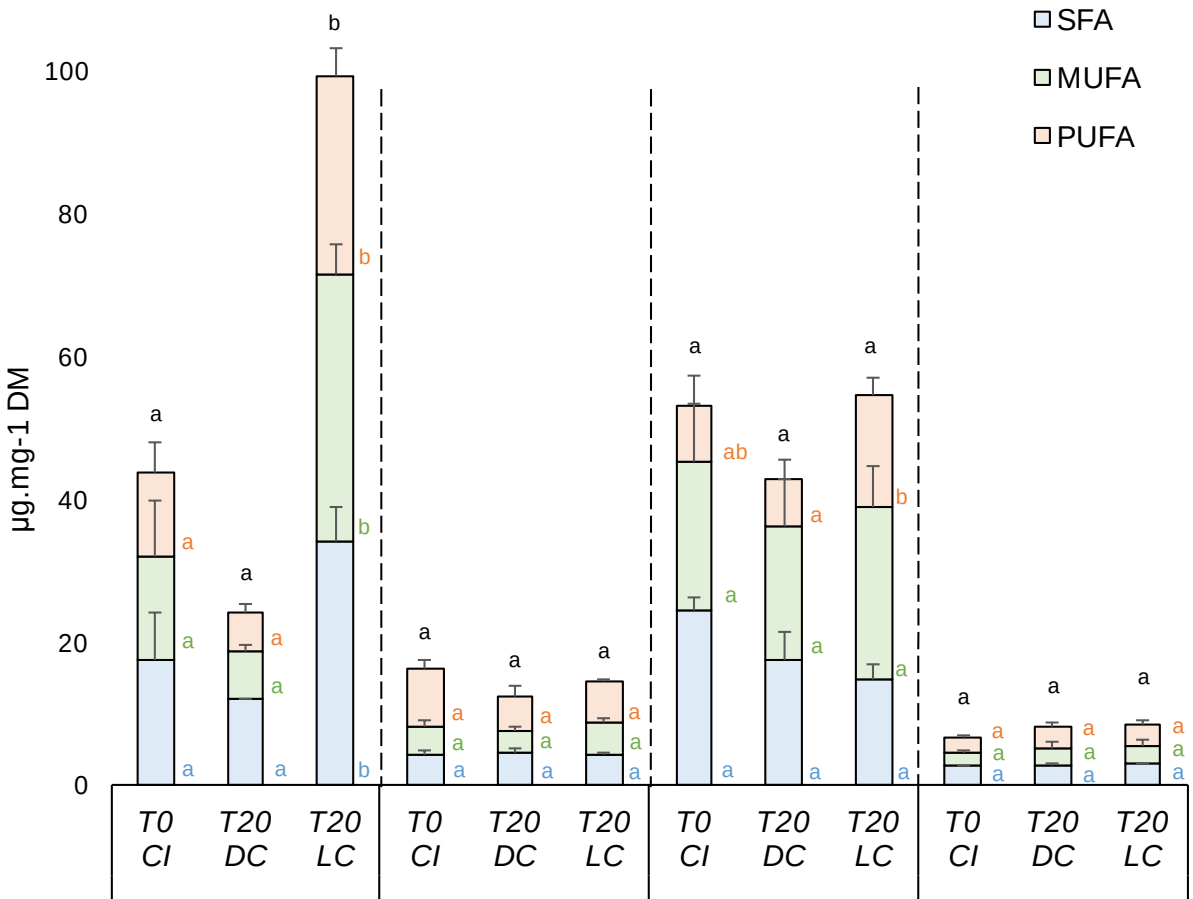
SFA
MUFA
PUFA
µg.mg-1 DM
0
20
40
60
80
100
T0 CI
T20 DC
T20 LC

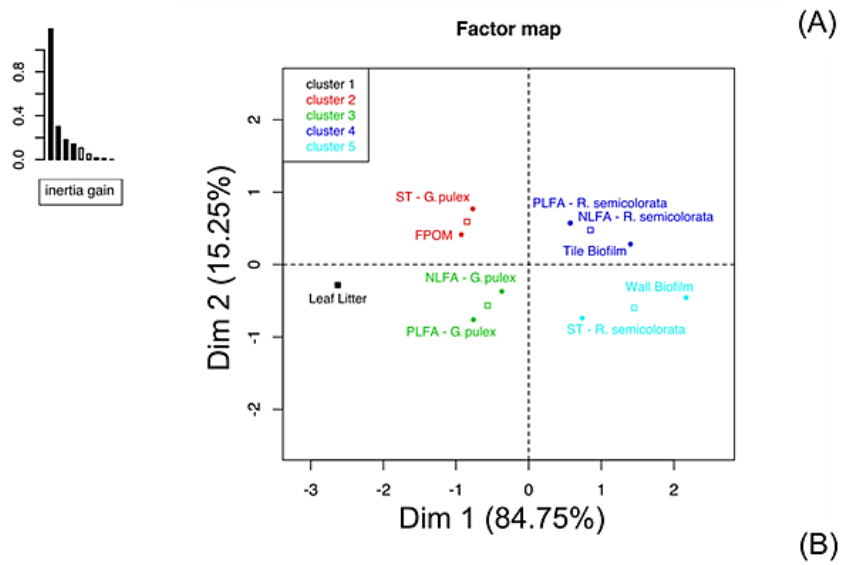
(A)
Factor map
inertia gain
0.0
0.4
0.8
cluster 1
cluster 2
cluster 3
cluster 4
cluster 5
ST - G.pulex
FPOM
PLFA - R. semicolorata
NLFA - R. semicolorata
Tile Biofilm
Leaf Litter
NLFA - G.pulex
PLFA - G.pulex
Wall Biofilm
ST - R. semicolorata
Dim 2 (15.25%)
Dim 1 (84.75%)
-3
-2
-1
0
1
2

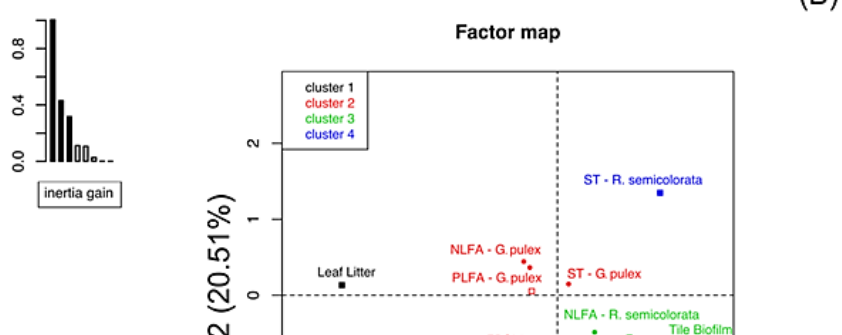
(B)
Factor map
inertia gain
0.0
0.4
0.8
cluster 1
cluster 2
cluster 3
cluster 4
ST - R. semicolorata
NLFA - G.pulex
PLFA - G.pulex
Leaf Litter
ST - G.pulex
NLFA - R. semicolorata
Tile Biofilm
Dim 2 (20.51%)
2
1
0